Arab J Geosci
DOI 10.1007/s12517-013-1162-4

ORIGINAL PAPER

Factors controlling the distribution of metals in intertidal mudflat sediments of Vaitarna estuary, North Maharashtra coast, India

Samida P. Volvoikar · G. N. Nayak

Received: 19 June 2013 / Accepted: 14 October 2013

Abstract Sediment cores collected from intertidal mudflats of Vaitarna estuary were investigated for distributions of sediment components, organic carbon, metals (iron, manganese, aluminum, copper, zinc, cobalt, nickel, and lead) in bulk sediments, as well as clay-sized fraction (<2 μm). Sorting of grain size under the influence of varying hydrodynamic energy conditions within Vaitarna estuary was discussed. Index of geoaccumulation indicated different levels of contamination for the studied metals at three locations. Pb and Zn were mainly found to be associated with clay fraction and showed exclusive lithogenic origin. While all the other metals showed signatures of anthropogenic origin in addition to that of lithogenic.

Keywords Bulk · Clay fraction · Estuary · Metals · Mudflat · Organic carbon

Introduction

Intertidal mudflat sedimentary environments within estuaries are depositing sites for the material brought from different sources, viz. terrestrial, marine, and atmospheric, and received from both natural and anthropogenic processes. The material includes sediment particles, organic matter, and associated metals. Metallic ions or ionic species accumulate through adsorption onto organic or mineral substrate, form organo-metallic complexes, and precipitate as (iron-) sulphides and/or insoluble oxy-hydroxides (Tribovillard et al. 2006). Within mudflats, layers of sediments get deposited over a period of time. Thus, surface sediments represent recent inputs while the layers below are older deposits reflecting changes in environmental conditions from past to present in a sequence. These deposited sediments can also act as source of heavy metals to the overlying waters due to changes in pH and redox condition. Postdepositional processes such as early diagenesis may play a significant role in metal remobilization, preservation, and enrichment within these sediments. Thus, elevated concentrations of metals within mudflat sediments may be the result of large input from natural/anthropogenic sources or due to diagenetic processes. The role of postdepositional processes in controlling the mobilization and vertical redistribution of accumulated metals in sediments were studied earlier by Skowronek et al. (1994), Singh and Nayak (2009), and Sundararajan and Natesn (2011). Concentration and vertical distribution of trace metals in sediments are controlled by factors such as particle size, mineral composition of sediments, carrier substances (e.g., hydroxides, carbonates, sulfides), sediment surface area, organic matter content, and effect of pH and Eh (Williams et al. 1994; Kljaković-Gašpić et al. 2009; Attia et al. 2012). Sediment grain size is one of the significant factors in influencing the concentration of heavy metals in estuarine sediments with metal concentrations normally enriched in fine-grained sediments (Nobi et al. 2010). Less mobilization of metals within fine-grained (<2 μm) sediments is stated to be due to sorption properties which depend on sediment characteristics (Matini et al. 2011; Rajkumar et al. 2012). However, metals are also known to accumulate in coarser sediments of the marine coastal environment (Aloupi and Angelidis 2002). The ability of heavy metals for mobilization depends on properties of the clay fraction of sediments. Thus, the study of metals associated with clay fraction is important to understand the role and ability of clay fraction to fix metals within the mudflat sediments. The present study has been carried

S. P. Volvoikar · G. N. Nayak (✉)
Department of Marine Sciences, Goa University, Taleigao Plateau, Goa 403206, India
e-mail: nayak1006@rediffmail.com

G. N. Nayak
e-mail: gnnayak@unigoa.ac.in

S. P. Volvoikar
e-mail: Samida2010@gmail.com

Published online: 10 November 2013

out with the aim to understand the depositional processes within the mudflat sediments of Vaitarna estuary. Attempt has also been made to study the distribution and association of metals within clay fraction and bulk sediment.

Study area

Vaitarna estuary is situated along northern coast of Maharashtra, India (Fig. 1). Both tide and wind dominate the regime, leading to well-mixed conditions almost throughout the year (Swamy 1994). Vaitarna estuary provides macrotidal environments. The river is one of the longest along Konkan coast with 154 km length. It has a drainage area of 3,647 km^2 that practically covers the entire northern sections of the Thane district with a number of tributaries, the most important being Pinjal, Surya, and Tansa. The Western Ghats in the region slope towards the west (Rastogi et al. 1997), leading Vaitarna and its tributaries to flow westwards. Vaitarna, Tansa, and Surya rivers are dammed towards their upper reaches to develop water reservoirs for power generation, irrigation, and water supply purposes. The tidal influence is observed up to 50 km from the mouth (Gazetteer 1982).

Geology of the study area

The study area is the part of the Deccan volcanic province (DVP) also known as Deccan Trap. The basaltic terrain has an undulating topography with landforms typical of the DVP (Shankar and Mohan 2006). The Deccan Trap basalts have uniform tholeiitic composition and are dark green to black volcanic rocks with a wide variety of textural character (Wensink 1973). In the Northwestern part, these tholeiitic basalts show notable picritic and alkali occurrences. They are largely microporphyritic with phenocrysts of plagioclase, subordinate augite, and rare olivine (Sano et al. 2001; Sen 2001).

Materials and methods

Three intertidal mudflat sediment cores from Vaitarna estuary were collected using hand-operated PVC corer. Core S4 of length 88 cm was collected near the mouth (19°28′56.3″N; 72°46′58.7″), core S9 having length of 52 cm represented lower middle estuary (19°31′23.9″N; 72°47′11.3″E), while core S7 of 66 cm length was collected from upper middle estuary (19°31′35.0″N; 72°53′37.5″E). Sampling stations were located using hand-held GPS. Soon after the collection, sediment core was sectioned at 2 cm interval with the help of a plastic knife. The subsamples were sealed in clean plastic bags, labeled, and kept in ice box. pH of subsamples was noted in the laboratory. Sediments were oven-dried at 60 °C. Pipette analysis was carried out following Folk (1968) to obtain sand/silt/clay components. Part of the dried samples was powdered and homogenized with the help of an agate mortar and pestle. Organic carbon (OC) was estimated following Walkey–Black method as given by Gaudette et al. (1974) using powdered samples. A known quantity of sediment was digested completely with $HF/HNO_3/HClO_4$ (7:3:1) acid mixture. Separated clay fractions from selected samples were also digested following the same procedure used for bulk sediments.

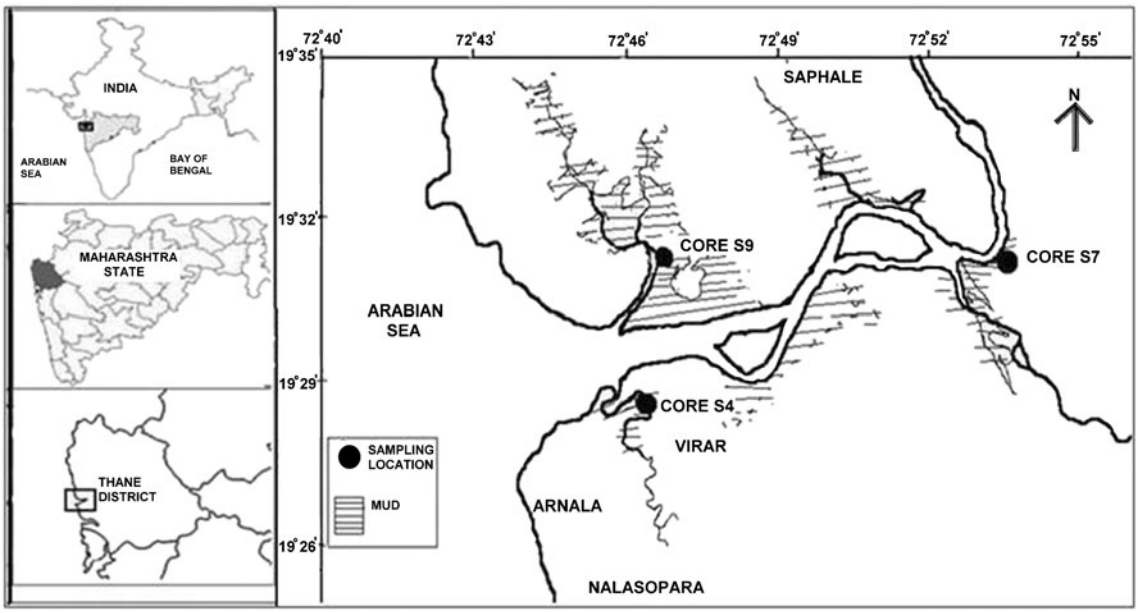

Fig. 1 Location of core samples collected from Vaitarna estuary, Maharashtra

Digested samples were then analyzed for bulk and clay chemistry, viz. iron (Fe), manganese (Mn), aluminum (Al), copper (Cu), zinc (Zn), cobalt (Co), nickel (Ni), and lead (Pb) by aspirating the sample solutions into the flame atomic absorption spectrophotometer (Varian AA240FS). Repeat analyses were carried out for all the metals after every ten samples in order to check the reproducibility of the instrument. All the reagents used in the present study are of analytical grade. Due care has been taken to avoid contamination during the time of sampling, storage, and analyses. The accuracy of the analytical procedure was assessed using certified reference standard from the Canadian National Bureau of Standards (BCSS-1). The recovery was 95 % for Mn and Co; 96 % for Fe, Cu, Ni, and Al; and 99 % for Zn and Pb. Statistical correlation analysis was carried out on the three cores using the STATISTICA software (StatSoft 1999). The ternary diagram proposed by Pejrup (1988) was used in order to understand the hydrodynamic condition of depositional environment under which the sediments of Vaitarna estuary were deposited. In this diagram, silt/clay axis has been divided into four parts distinguishing four hydrodynamic groups (I–IV) between the silt and clay end members. These groups represent the energy gradient from lower (clay-dominated muds) to higher (silt-dominated muds) energy levels. The energy also decreases from sandy end member to muddy end member (A to D) for the four groups. Geoaccumulation index as proposed by Müller (1969) was calculated as:

$$I_{geo} = \log_2 C_n / 1.5\, B_n$$

Where C_n is the concentration of the studied element and B_n is the geochemical background value taken from global average shale for element n. The background metal concentration is multiplied with 1.5 to take into account the natural fluctuation of the element in the background (Haris and Aris 2012). Modified sequential extraction procedure (Dessai and Nayak 2009) proposed by Tessier et al. (1979) was used for a selected subsample of core S7 in order to understand association of metals with different sedimentary fractions and to understand their origin.

Results and discussion

Sediment components

In the core collected towards the mouth (S4), sand percentage was relatively high as compared to the other two locations, whereas clay and silt percentage was higher in core collected towards the lower middle estuary (S9) and the upper middle estuary (S7), respectively (Table 1). The results of one-way ANOVA indicated significant ($p < 0.05$) difference in sand, silt, and clay percentages between and within the three cores ($p = 0.00$). Large variation in the distribution of sand was observed from bottom to surface in core S4 with overall decreasing trend (Fig. 2a). The variation in sand percentage was largely compensated by distribution of clay. Silt also showed opposite distribution pattern to that of sand especially in the upper 30 cm. In core S9, sand percentage was almost constant from bottom to the surface of the core except between 44 and 30 cm wherein sand increased slightly with a small peak at 38 cm depth and with relatively lower values above 16 cm (Fig. 2b). Clay percentage compensated for the variation in silt. Towards the upper middle estuary (core S7), sand was almost constant from bottom to surface of the core except between 58 and 42 cm wherein relatively higher sand percentage with a peak at 50 cm depth was observed (Fig. 2c). Silt showed opposite trend to that of clay; large variations from bottom to a depth of around 24 cm were noted, above which both silt and clay showed almost constant trend up to surface. The higher average percentage of clay in core

Table 1 Range and average values of studied parameters within bulk sediments

	Sand (%)	Silt (%)	Clay (%)	OC (%)	Al (%)	Fe (%)	Mn (ppm)	Cu (ppm)	Zn (ppm)	Co (ppm)	Ni (ppm)	Pb (ppm)
Core S4												
Max	59.3	47.6	55.4	2.41	12.9	12.5	1,518	141	172	106	169	83
Min	14.5	11.9	15.8	0.70	7.7	7.4	887	96	123	71	131	29
Avg	39.3	26.6	34.0	1.38	10.2	9.7	1,115	122	150	92	153	60
Core S9												
Max	27.8	75.4	66.8	5.85	11.2	11.8	1,274	143	170	93	143	143
Min	3.71	26.4	8.44	0.84	5.5	7.9	714	81	118	65	111	58
Avg	11.5	37.6	50.8	1.70	9.3	10.2	1,100	117	152	80	130	95
Core S7												
Max	48.8	52.0	72.5	2.01	11	11.6	2,264	192	186	101	146	111
Min	2.42	24.9	16.6	0.89	6.1	6.4	1,256	129	141	65	116	69
Avg	11.3	39.5	49.2	1.28	9.1	9.4	1,734	148	157	83	130	86

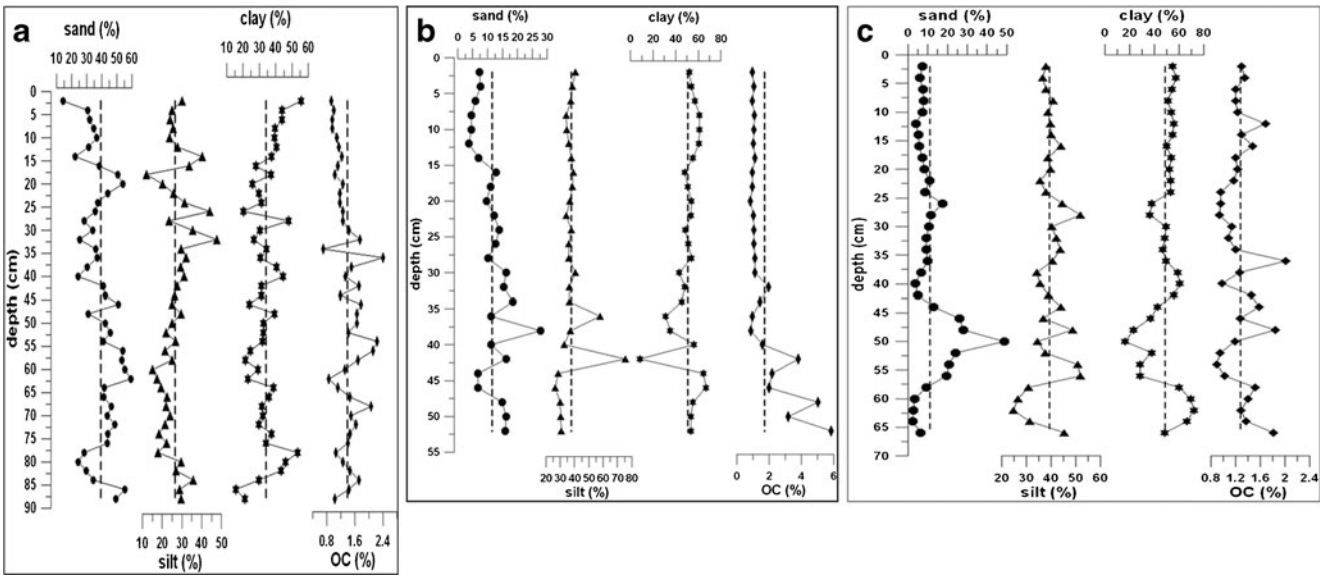

Fig. 2 Depth distribution of sediment components and organic carbon: **a** core collected towards the mouth (core S4); **b** core collected from the lower middle estuary (core S9); **c** core collected from the upper middle estuary (core S7)

S9 collected from relatively sheltered region may be attributed to comparatively low tidal energy regime promoting transport of mainly fine particulates to this area (O'Reilly et al. 1995). The higher sand percentage near the bottom and increase in clay component towards surface in all the three cores reflected prevailing hydrodynamics. The large variations in grain size distribution may be because of changes in material supply and processes involved at the site of deposition. Dredging activities must have also contributed for the distribution of sediment components (Huaiyang et al. 2004). It is a known fact that fine-grained sediments are easily kept in suspension and they need calm conditions to settle from the water column (Dolch and Hass 2008). Further, the data points on the ternary diagram (Fig. 3) indicated that the sediments of Vaitarna estuary have deposited under less violent to relatively violent hydrodynamic conditions. It also indicated a gradual decrease in grain size from lower estuary to upper middle estuary, indicating the grain size sorting in response to changes in hydrodynamic or energy conditions. Siraswar and Nayak (2011) also observed similar changes in energy conditions and progressive sorting of sediments by tidal currents in their study. Zhang et al. (2002) reported that in the intertidal flats, hydrological dynamics control the grain size distribution from seaward to landward, and grain size in turn controls the distribution of the element concentrations. Sediment grain size has also been found to be one of the main factors

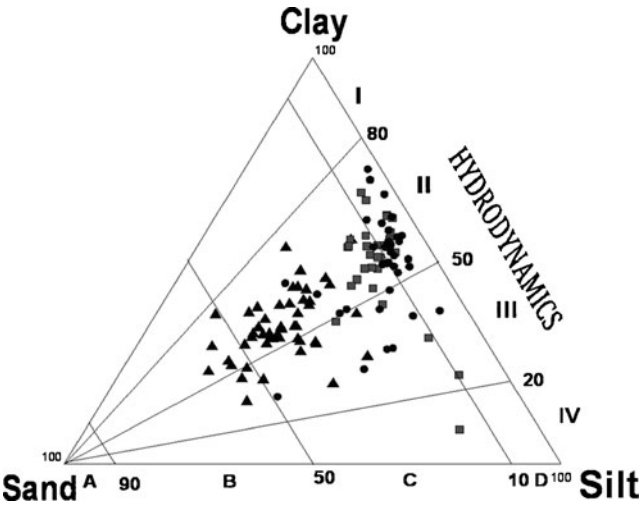

Fig. 3 Ternary diagram showing deposition of sand, silt, and clay under varying hydrodynamic energy conditions after Pejrup (1988). *Triangles* represent core collected towards the mouth, *squares* indicate core collected from the lower middle estuary, and *circles* represent core collected from the upper middle estuary

Table 2 Result of one-way ANOVA (the mean difference is significant at the 0.05 level)

	Core S4 vs core S9	Core S9 vs core S7	Core S4 vs core S7
Sand	*	***	*
Silt	*	***	*
Clay	*	***	*
OC	***	***	***
Al	*	***	*
Fe	***	*	***
Mn	***	*	*
Cu	***	*	*
Zn	***	***	*
Co	*	***	*
Ni	*	***	*
Pb	*	***	*

*$p<0.05$; **$p=0.05$; ***$p>0.05$

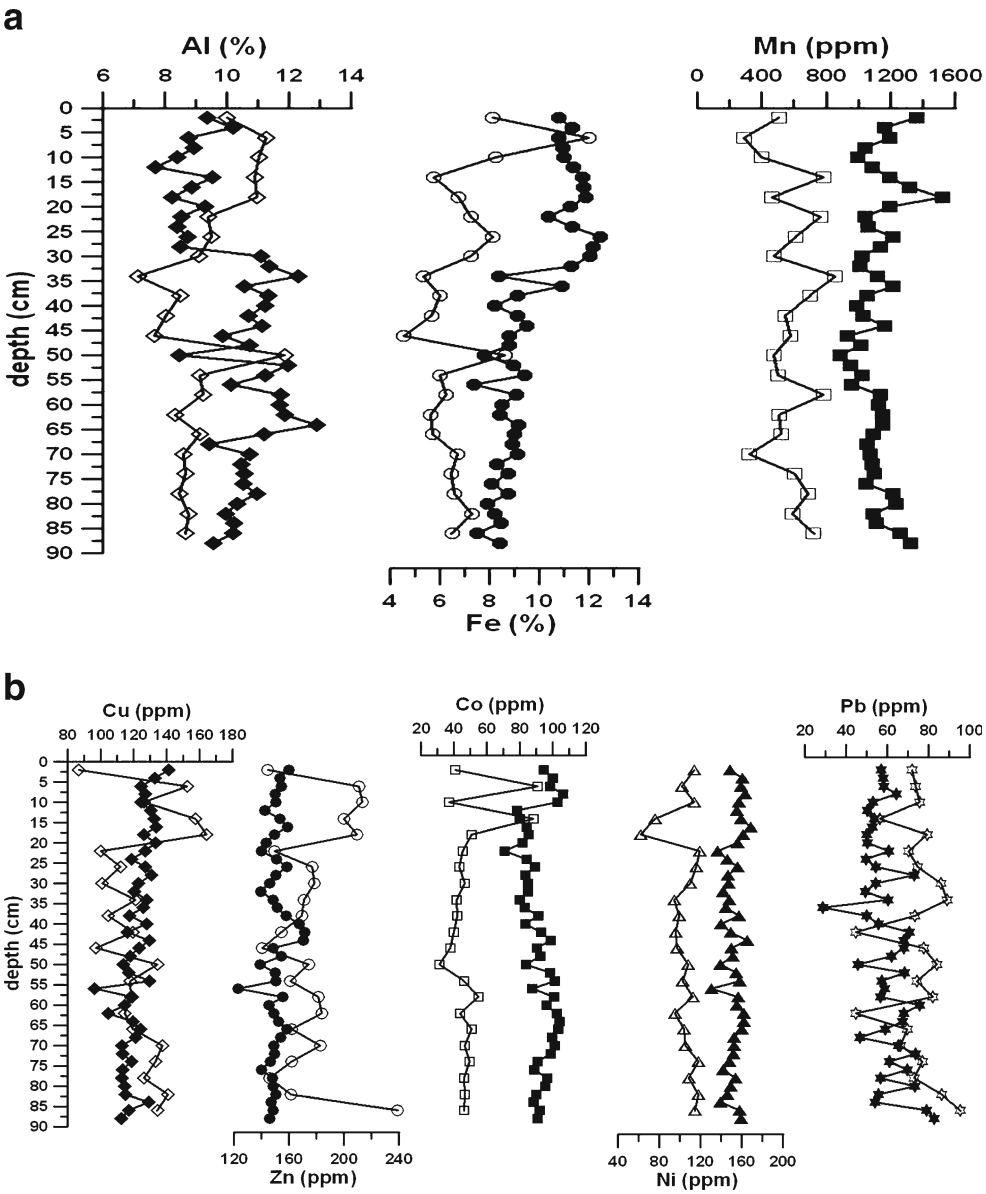

Fig. 4 Depth distribution of metals **a** Al, Fe, and Mn; **b** Cu, Zn, Co, Ni, and Pb in core collected towards the mouth. *Filled symbols* represent metals in bulk sediment. *Empty symbols* represent metals in clay fraction of sediment

controlling the distribution of organic matter (Venkatramanan et al. 2013).

Organic carbon

OC in core S4 (Fig. 2a) showed fluctuating trend from bottom to 32 cm, above which it decreased gradually, whereas in core S7 (Fig. 2c) OC was almost constant from bottom to surface with few peaks. It is noteworthy to mention here that in core S9 (Fig. 2b) OC exhibited large variations with much higher values towards the lower portion, i.e., from bottom to a depth of 40 cm. The high OC obtained towards the bottom of the core pointed towards addition of high proportion of terrestrial organic matter which is known to include a higher proportion of biologically resistant organic compounds which are less susceptible to biological degradation leading to a better preservation (Álvarez-Iglesias et al. 2006). Above 40 cm, OC was low and almost constant indicating presence of labile organic matter of marine origin. The result of one-way ANOVA however indicated no significant difference between OC concentrations at the three locations ($p = 0.08$).

Al, Fe, and Mn in bulk sediment

The average percentages of metals in all the three cores when compared indicated relatively high Al, Fe, and Mn concentrations in core collected near the mouth (core S4), lower middle estuary (core S9), and upper middle estuary (core S7), respectively (Table 1). The results of one-way ANOVA analysis indicated all the three major elements to show significant difference in distribution between and within the three cores. Wherein, Al and Mn showed significant

difference between cores S4 and S7, while Fe indicated no significant difference between the two cores. Fe and Mn showed significant difference between cores S9 and S7 (Table 2), while Al showed no significant difference between these two cores. However, no significant difference was observed between cores S9 and S4 for the three metals. Near the mouth (core S4), Al showed large fluctuating trend between 68 and 28 cm depth with a lower value at 50 cm (Fig. 4a). Above 28 cm, Al was relatively lower and showed an increasing trend towards the surface. At the lower middle estuary (core S9), Al fluctuated with overall increasing trend but with relatively lower values below 30 cm depth. Above 30 cm, Al was almost constant except for a large decrease at 22 cm depth (Fig. 5a). Core S7 collected at the upper middle estuary indicated fluctuations with overall decreasing trend for Al from bottom to a depth of 18 cm (Fig. 6a). Above 18 cm, sudden and large decrease in Al concentration followed by an increase towards the surface was noted which is similar to trend in core S4. Aluminum is a typical lithogenic element and is considered to be an important erosion indicator suggesting terrigenous input (Shi et al. 2010) to the sediments. It is therefore considered to act as a "proxy" for the clay content (Abrahim and Parker 2008). However in the present study, Al and clay did not show much similarity in distribution pattern especially in core S4 and S7, thus indicating association of Al with other sedimentary components (silt and sand) in addition to that of clay.

Vertical profile of Fe in core S4 showed an increasing trend from bottom to a depth of around 32 cm with minor variations (Fig. 4a). Above 32 cm, Fe maintained an overall high percentage as compared to the lower depths and showed decreasing trend from 20 cm to surface. Fe showed similar

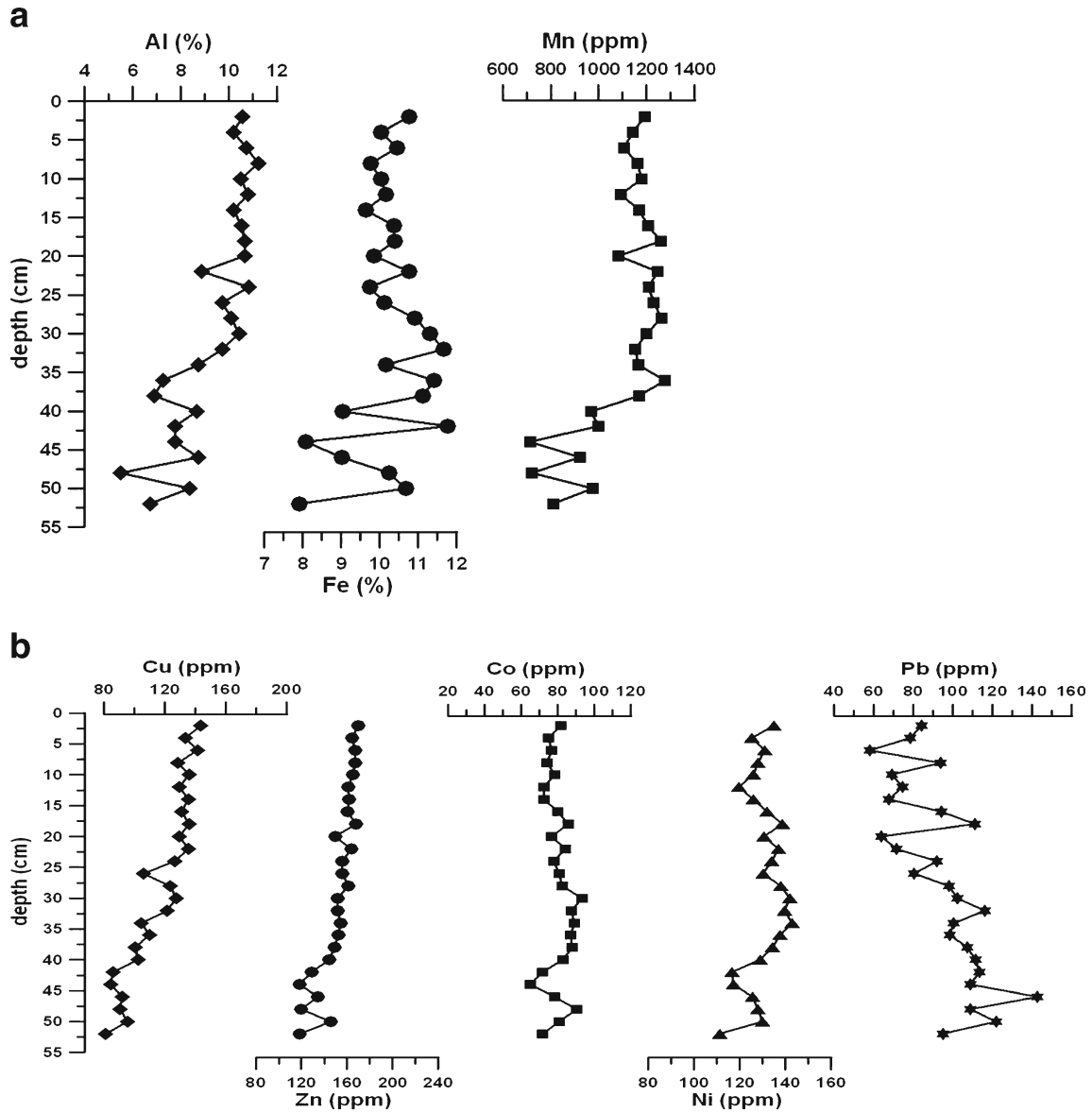

Fig. 5 Depth distribution of metals **a** Al, Fe, and Mn; **b** Cu, Zn, Co, Ni, and Pb in core collected from the lower middle estuary

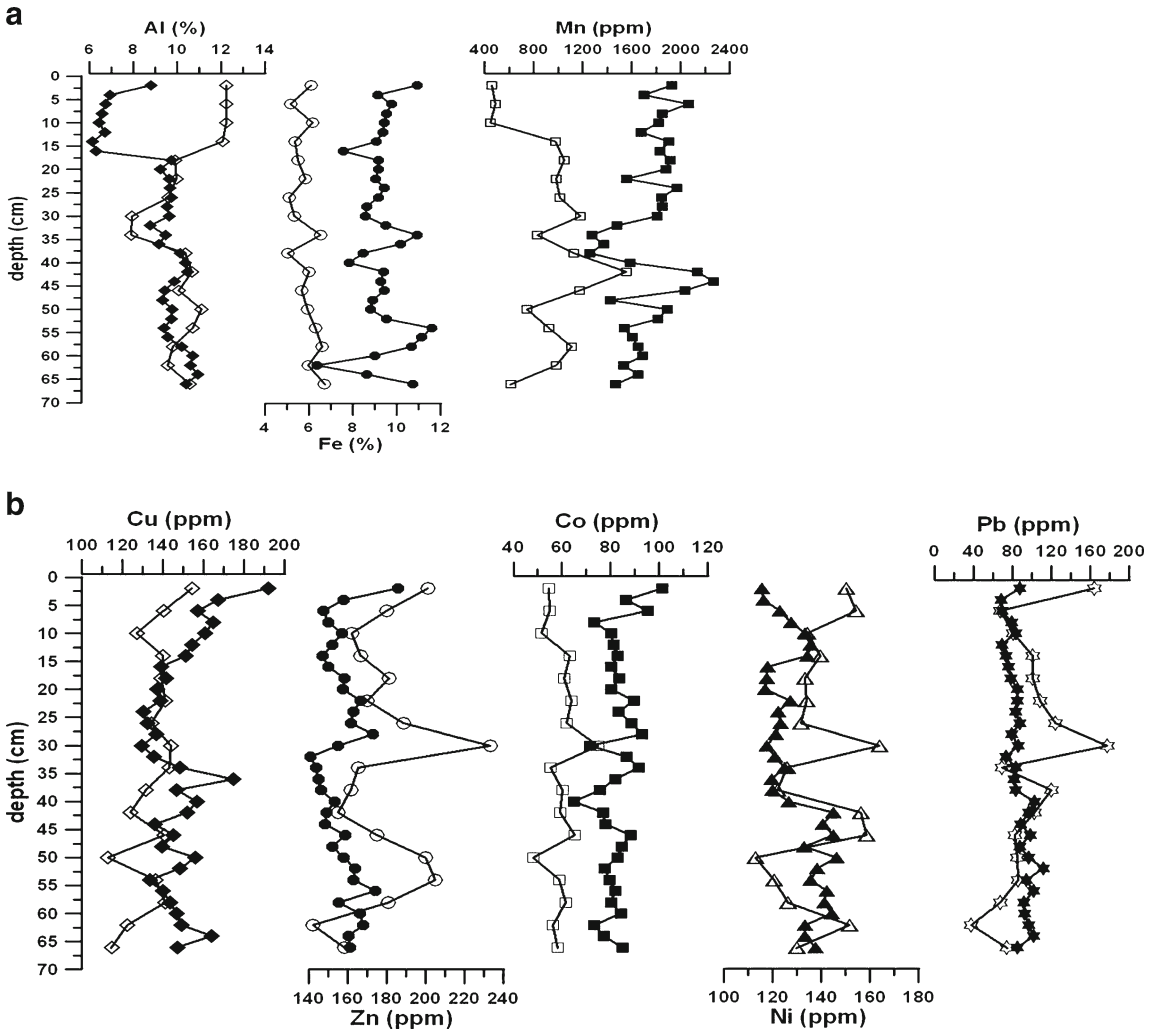

Fig. 6 Depth distribution of metals **a** Al, Fe, and Mn; **b** Cu, Zn, Co, Ni, and Pb in core collected from the upper middle estuary. *Filled symbols* represent metals in bulk sediment. *Empty symbols* represent metals in clay fraction of sediment

distribution pattern to that of Al between 80 and 42 cm. Not much variation in Mn concentration was noted from bottom to 56 cm except for gradual decrease. Above 56 cm, Mn value fluctuated with overall increasing trend and a peak at 18 cm depth. Mn distribution matched Al between 58 and 42 cm. In core S9, Fe showed larger fluctuations from bottom to 26 cm depth above which it remained almost constant (Fig. 5a). Mn also showed fluctuating trend with relatively lower values from bottom to a depth of 38 cm. Above 38 cm, Mn was almost constant and showed a slight decrease at 20 cm depth. Mn distribution indicated similarity with Al from bottom to 44 cm depth. At the upper middle estuary (core S7), Fe showed large variations from bottom to 52 cm and 42–30 cm (Fig. 6a). Both Fe and Al showed large increase at the surface and a sudden decrease at 16 cm depth. Mn showed an overall increasing trend with large variations between 50 and 30 cm. The similarity in distribution pattern of Fe and Mn with Al at various depths in these cores represented portion of alumino-silicate mineral bound fraction and/or weathered material of terrestrial source rock. Fe and Mn are redox-sensitive elements and their distribution pattern has been used previously to understand early diagenetic processes (Cundy and Croudace 1995; Spencer 2002; Ruiz-Fernández et al. 2007; Caetano et al. 2009). In the partly reduced sediment layers, dissolution of Fe-Mn oxyhydroxides takes place producing Fe^{+2} and Mn^{+2} species. Large increase in Fe and Mn concentration in core S4 can therefore be attributed to migration and reprecipitation of Fe^{+2} and Mn^{+2} species as oxy-hydroxides near the oxic–suboxic interface. While the presence of distinct Fe and Mn peaks in core S7, i.e., at 54 and 44 cm, respectively, must be the result of their difference in oxidation. Higher stability of Fe oxyhydroxides under mildly reducing conditions and faster oxidation kinetics of Fe^{+2} compared to Mn^{+2} occasionally leads to diagenetic enrichment of Fe at greater depth as compared to diagenetic Mn enrichment (Zwolsman et al. 1993). However, additional peak of Fe at 34 cm depth in this core was probably a result of repetition of diagenetic reactions (Soto-Jiménez and Páez-

Table 3 Correlation between sand, silt, clay, organic carbon, and metals in core S4

	Sand	Silt	Clay	OC	pH	Fe	Mn	Al	Cu	Zn	Co	Ni	Pb
Sand	1.00												
Silt	−0.55	1.00											
Clay	−0.74	−0.16	1.00										
OC	0.19	0.13	−0.32	1.00									
pH	−0.01	−0.09	0.09	−0.24	1.00								
Fe	−0.35	*0.34*	0.14	−0.27	−0.07	1.00							
Mn	−0.05	−0.06	0.10	−0.43	0.21	*0.31*	1.00						
Al	0.15	−0.08	−0.11	0.17	−0.04	−0.50	−0.20	1.00					
Cu	−0.47	*0.32*	*0.30*	−0.25	0.06	*0.66*	*0.31*	−0.32	1.00				
Zn	−0.30	0.15	0.23	−0.16	−0.34	0.16	0.22	0.15	*0.43*	1.00			
Co	0.18	−0.38	0.09	−0.01	0.06	−0.27	−0.04	*0.38*	−0.23	0.29	1.00		
Ni	0.13	−0.18	−0.02	−0.41	0.07	0.29	*0.47*	0.04	0.27	*0.47*	*0.51*	1.00	
Pb	*0.30*	−0.28	−0.13	−0.29	0.02	−0.43	0.04	0.26	−0.33	0.02	*0.34*	0.18	1.00

Values in italics are significant at $p < 0.05$, $N = 44$

Osuna 2008). While in core S9, though the distribution pattern of Fe and Mn was almost similar, no such maxima or peak values were noted. The similarity in distribution pattern of Fe with Mn in core S4 and more precisely in core S9 therefore indicated association of the geochemical matrix between the two elements (Jonathan et al. 2010).

Trace metals in bulk sediment

The average concentration of metals indicated variation in the spatial distribution of metals with relatively high concentration of Co and Ni towards the mouth (core S4), Pb in core collected from the lower middle estuary (core S9) while high concentration of Cu and Zn in upper middle estuary (core S7). The results of one-way ANOVA analysis indicated all the studied trace metals to show significant difference in distribution between and within the three cores; wherein, all the metals showed significant difference between cores S4 and S7 (Table 2). Cu showed significant difference between cores S9 and S7, while all the other metals namely Zn, Co, Ni, and Pb showed no significant difference between these two cores. Co, Ni, and Pb showed significant difference between cores S9 and S4, whereas other metals namely Cu and Zn indicated no significant difference. Vertical distribution pattern of Cu indicated an overall increasing trend with fluctuations from bottom to surface in the core S4 maintaining relatively higher values within upper six centimeters (Fig. 4b). Zn was almost constant from bottom

Table 4 Correlation between sand, silt, clay, organic carbon, and metals in core S9

	Sand	Silt	Clay	OC	pH	Fe	Mn	Al	Cu	Zn	Co	Ni	Pb
Sand	1.00												
Silt	0.17	1.00											
Clay	−0.59	−0.89	1.00										
OC	0.29	−0.01	−0.13	1.00									
pH	−0.12	0.02	0.04	−0.24	1.00								
Fe	0.34	*0.59*	−0.64	−0.27	0.10	1.00							
Mn	−0.00	0.29	−0.23	−0.77	0.02	*0.58*	1.00						
Al	−0.54	−0.07	0.30	−0.71	0.08	0.10	*0.62*	1.00					
Cu	−0.45	−0.01	0.22	−0.73	0.05	0.31	*0.73*	*0.83*	1.00				
Zn	−0.32	0.04	0.12	−0.82	0.08	*0.40*	*0.87*	*0.79*	*0.90*	1.00			
Co	*0.54*	−0.01	−0.24	−0.14	−0.27	*0.57*	0.36	−0.16	0.09	0.18	1.00		
Ni	0.29	−0.01	−0.13	−0.55	−0.11	*0.59*	*0.67*	0.27	*0.44*	*0.54*	*0.82*	1.00	
Pb	*0.41*	−0.02	−0.17	*0.40*	−0.23	0.01	−0.38	−0.48	−0.66	−0.54	0.26	0.03	1.00

Values in italics are significant at $p < 0.05$, $N = 26$

Table 5 Correlation between sand, silt, clay, organic carbon, and metals in core S7

	Sand	Silt	Clay	OC	pH	Fe	Mn	Al	Cu	Zn	Co	Ni	Pb
Sand	1.00												
Silt	0.26	1.00											
Clay	−0.88	−0.69	1.00										
OC	−0.15	−0.08	0.15	1.00									
pH	0.16	0.03	−0.13	−0.11	1.00								
Fe	0.16	*0.44*	−0.34	0.03	0.04	1.00							
Mn	0.09	−0.01	−0.06	−0.18	−0.35	−0.09	1.00						
Al	0.15	−0.21	−0.01	−0.06	*0.59*	−0.02	−0.21	1.00					
Cu	−0.18	−0.32	0.29	0.32	−0.38	0.13	−0.03	−0.27	1.00				
Zn	0.11	−0.02	−0.07	−0.32	−0.09	0.11	0.12	0.29	0.11	1.00			
Co	0.13	0.23	−0.21	−0.00	−0.29	*0.43*	0.10	−0.18	0.16	0.31	1.00		
Ni	*0.39*	−0.13	−0.23	0.15	*0.39*	0.15	0.15	0.28	−0.09	0.07	−0.20	1.00	
Pb	*0.37*	−0.19	−0.19	−0.21	*0.48*	0.00	−0.02	*0.69*	−0.05	*0.38*	−0.37	*0.56*	1.00

Values in italics are significant at $p < 0.05$, $N = 33$

to 58 cm, above which it showed fluctuating trend up to the surface. Co maintained relatively higher values above 12 cm depth. It also showed similar point to point variation pattern to that of Zn from bottom to 12 cm depth. Similarly, the variation in distribution pattern of Ni was almost the same as that of Co. All the metals except Pb showed a prominent decrease at 56 cm depth. Pb had its maximum concentration at the bottom and varied with fluctuating trend up to 26 cm depth, followed by a gradual increase towards the surface. Pb exhibited inverse relationship with Fe, whereas most of the other metals showed similarity with Fe and Mn at various depths.

In core S9 collected from the lower middle estuary, all the metals except Pb showed similar distribution pattern especially Zn, Ni, and Cu to that of Mn and Al, while Co showed similarity with Fe (Fig. 5b). Pb showed higher values towards the bottom of the core similar to that of OC. In core S7 collected at the upper middle estuary, fluctuating trend of Cu was noted up to 32 cm depth with a peak at 36 cm which is similar to OC (Fig. 6b). Above 32 cm, Cu increased gradually towards the surface of the core. Zn decreased gradually from bottom to 32 cm depth followed by an increase up to 28 cm and a decreasing trend till 6 cm depth. Above this, Zn showed a large increase towards the surface. Less fluctuation in Co concentration was observed from bottom to 8 cm depth, except between 46 and 28 cm where Co showed relatively larger variations. Large increase in Co concentration was observed above 8 cm depth. The point to point variation pattern in Co concentration agreed with that of Fe below 28 cm depth, it also showed similarity with Cu and Zn at some depths. Pb was almost constant from bottom to surface of the core and exhibited maximum concentration at 52 cm depth. Ni showed a gradual decreasing trend from bottom to surface with peak value at 50 cm, corresponding to a similar increase in Cu and sand percentage at this depth. The variation in distribution pattern of Ni matched Co below 16 cm depth.

The inter-element relationships observed on the basis of vertical distribution of metals in cores S4, S9, and S7 suggested that they are derived from the same source and/or have undergone similar postdepositional changes (Zwolsman et al. 1996; Sullivan and Taylor 2003; Wang and Zhai 2008). Lack of significant differences in distribution of most of the metals between cores S9 and S7 and between core S9 and S4 further provided support for their similar source of input. Thus to establish interrelationships between the studied parameters and to identify their sources, correlation coefficients were further determined (Mukherjee et al. 2009). Correlation analysis indicated Cu to show strong positive association with Fe, Mn, and Zn in core collected towards the mouth (core S4) (Table 3). Ni was found to be associated with Mn, Zn, and Co; Co in turn was found to be associated with Pb. Whereas, in core collected towards the lower middle estuary (core S9), most of the metals were strongly positively correlated with Fe and Mn (Table 4) except for Pb, indicating Fe-Mn oxyhydroxide to be the major phase controlling the distribution of metals within this core. Also, association of Cu, Zn, and Mn with Al probably indicated their terrestrial origin. While towards the upper middle estuary (core S7), only one metal, i.e., Co, showed good correlation with Fe (Table 5) indicating association of Co with ferric hydroxides. Lack of significant correlations among concentrations of most of the trace metals and Fe and Mn in core S7 confirmed that their distribution in this core was not dependent on redox conditions (Ruiz-Fernández et al. 2009). Fe-Mn oxyhydroxide, however, was one of the major controlling factors for the distribution of most of the metals within cores S9 and to some extent in S4 of Vaitarna estuary. In case of core S4 collected towards the mouth where sand percentage was relatively higher, infiltration of oxygenated water through the sandy sediments must have exerted a significant control over the development of diagenetic

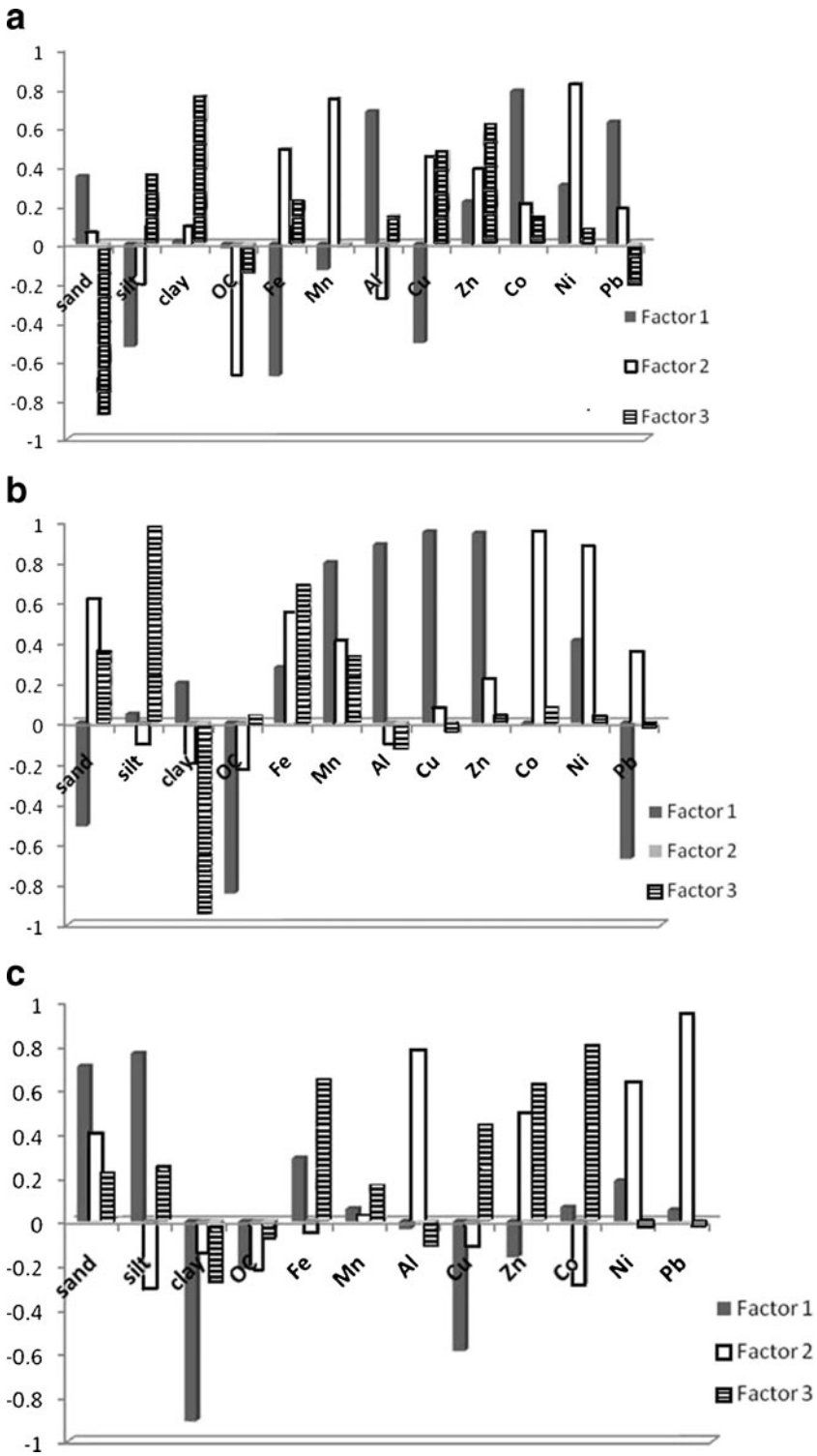

Fig. 7 R-mode factor analysis for **a** core collected towards the mouth; **b** core collected from the lower middle estuary; **c** core collected from the upper middle estuary

Fe phases (Ohmsen et al. 1995). Also, most of the metals did not show good correlation with clay and OC (Tables 3, 4, and 5) indicating their less association. Fe and Pb showed strong positive correlation with silt and sand, respectively, at all the three stations. Co and Ni were also associated with sand fraction in core S9 and S7, respectively, indicating role of coarser fraction in distribution of these metals.

Factor analysis was also carried out on the studied parameters to understand the sources of metals in sediments of Vaitarna estuary. The three factors drawn account for 62, 85, and 57 % total variance for core S4, S9, and S7, respectively. Factor loadings with varimax rotation, having eigen values greater than one, are shown in Fig. 7a–c. The results of factor analyses were in good agreement with that of

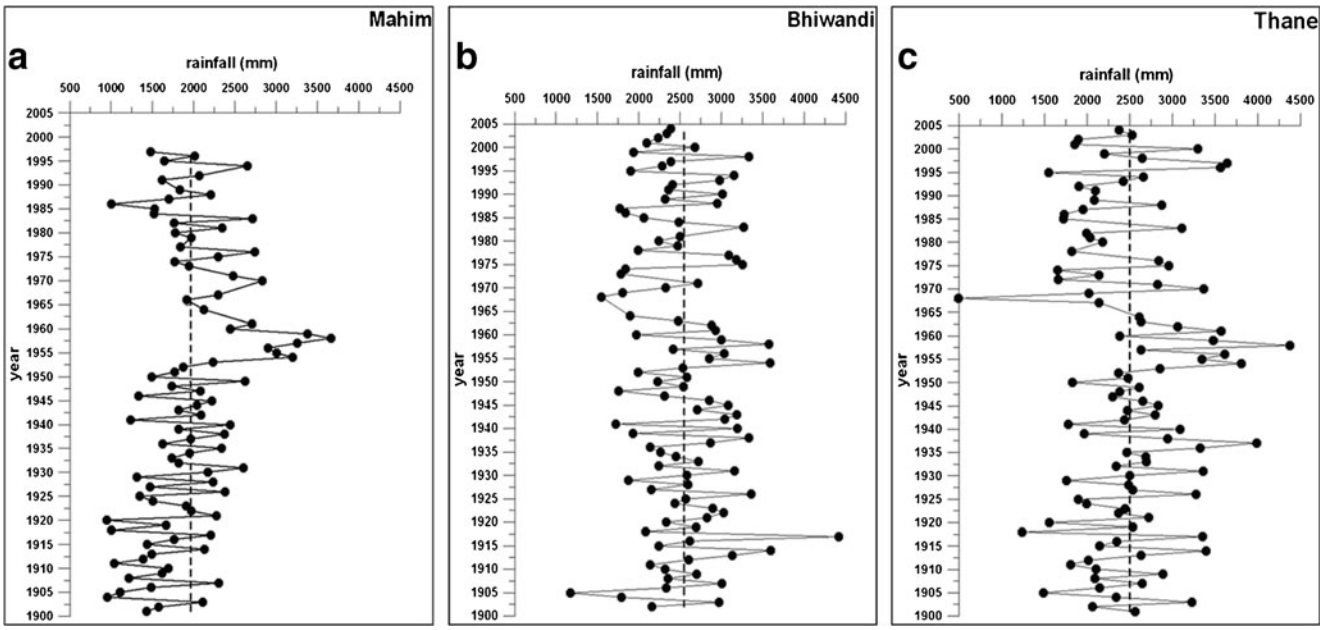

Fig. 8 Rainfall data of last 100 years for three different stations in Thane district

correlation analyses. For core collected towards the mouth (core S4), the positive loadings of Al, Co, Pb, and sand together with minor loadings of Zn and Ni in factor 1 indicated association of these metals with coarser size fraction. Silt, Fe, and Cu were negatively loaded and therefore indicated association of Fe with silt and adsorption of Cu onto Fe-oxide precipitate. In factor 2, positive loadings of Fe, Mn, Cu, Zn, and Ni indicated adsorption of these metals onto Fe-Mn oxy-hydroxide precipitate. However, negative loading of OC further supported the negligible influence of organic matter on metal distribution. Metals showed some association with clay in factor 3.

For the core collected from lower middle estuary (core S9), first factor showed positive loadings of Mn, Al, Cu, Zn, and to a lesser extent Fe and Ni. This indicated association of metals with Fe-Mn oxy-hydroxide precipitate. While negative loadings of OC, Pb and sand indicated their different source. Factor 2 showed positive loadings of Co and Ni which were found to be associated with Fe, Mn, and sand. Factor 3 indicated positive loadings of silt and Fe and minor loadings of sand and Mn.

For core collected towards the upper middle estuary (core S7), factor 1 showed positive loadings of sand, silt, and Fe. Whereas clay and Cu were negatively loaded, indicating difference in metal associations. Factor 2 indicated positive loadings of Al, Zn, Ni, Pb, and sand, pointing towards metals derived from land source. While silt and OC were found to control the distribution of Co. Factor 3 indicated positive loadings of Fe, Zn, Co, and Cu.

Enrichment of metals towards the surface of all the three cores indicated either additional input during recent years or diagenetic remobilization. It is known that reductive dissolution of Fe-Mn hydroxides in the lower suboxic zone releases dissolved Mn(II) and Fe(II), and associated trace metals to pore waters (Koretsky et al. 2007). The Mn(II) and Fe(II) together with other metals must have diffused and redistributed within the upper sediments and re-precipitated within the oxic zone thus scavenging porewater trace metals towards the surface of the cores. However, in core S7, metals did not show much similarity with the distribution pattern of Fe and Mn. Also, in all the three studied cores, metals did not show sharp peak values corresponding to Fe and Mn. Koschinsky (2001) stated that solid element distribution does not always correspond exactly to the present redox zonation. Some metals may not follow the strict pattern of redox zonation, as they may have several reactions characteristics and/or only a small fraction may be diagenetically reactive. Higher average concentration and enrichment of Co and Ni in core S4 and Cu, Zn, and Co in core S7 within upper few centimeters must therefore have reflected enhanced

Table 6 I_{geo} class showing sediment quality (Müller 1969)

I_{geo}	I_{geo} classes	Sediment quality
<0	0	Unpolluted
0–<1	1	Unpolluted and moderately polluted
1–2	2	Moderately polluted
2–3	3	Moderately to highly polluted
3–4	4	Highly polluted
4–5	5	Highly to very highly polluted
>5	6	Very highly polluted

Table 7 Average values of I_{geo} in cores collected from Vaitarna estuary

	Avg. I_{geo} values in core S4	Sediment quality	Avg. I_{geo} values in core S9	Sediment quality	Avg. I_{geo} values in core S7	Sediment quality
Fe	1.6	Moderately polluted	1.7	Moderately polluted	1.6	Moderately polluted
Mn	1	Moderately polluted	0.9	Unpolluted to moderately polluted	1.6	Moderately polluted
Cu	2	Moderately polluted	1.9	Moderately polluted	2.3	Moderately to highly polluted
Zn	1.2	Moderately polluted	1.3	Moderately polluted	1.3	Moderately polluted
Co	2.8	Moderately to highly polluted	2.7	Moderately to highly polluted	2.7	Moderately to highly polluted
Ni	1.7	Moderately polluted	1.5	Moderately polluted	1.5	Moderately polluted
Pb	2.1	Moderately to highly polluted	2.8	Moderately to highly polluted	2.7	Moderately to highly polluted

anthropogenic addition in recent years as well. Among the studied metals, Zn was noticed to show an increase in concentration (Table 1) from mouth to upper middle estuary (i.e., core S4<core S9<core S7). Thus in the present study, Zn concentration seems to have been controlled by grain size which in turn was controlled by hydrodynamic processes. As shown in Fig. 1, core S4 was collected from a narrow subchannel near the mouth of Vaitarna esuary and was affected mainly by marine processes. However, this channel further extends southwards into a populated and urbanized region. Core S7 was collected from a region which is directly connected to major rivers on its upper reaches. While no major tributaries/rivers join the creek of Vaitarna estuary from which core S9 has been collected. The surrounding region of this creek is mainly comprised of agricultural land and village areas with less population. Thus, the higher average concentration of Pb noticed in core S9 (Table 1) as compared to cores S4 and S7 does not represent anthropogenic input. This is also supported by depth-wise distribution pattern which showed a decreasing trend towards the surface. Higher concentration of metals at the other two locations however reflected additional input in recent years probably of anthropogenic origin brought in by tributaries.

The protected area of core S9 must have facilitated the deposition of sediments under relatively less dynamic environment systematically recording changes in metal input. Thus, observed gradual increasing trends of Cu and Zn similar to that of Al and Mn and opposite to that of organic carbon suggested gradual change in depositional conditions facilitating enrichment of these metals at this location from past to present. Reduced freshwater inflow over a period of time is known to be one of the factors which may contribute to the gradual accumulation of metals within an estuary (Ruiz and Saiz-Salinas 2000). However, as discussed earlier, this portion of the estuary does not receive freshwater from major rivers, and sediment deposition seems to be mainly controlled by tidal processes at this location. Also as this portion of the estuary falls mainly under pristine region, increased anthropogenic activities does not justify for gradual metal enrichment though there can be some input from agriculture. Correlation and factor analysis also have identified source of these metals (Cu, Zn, Mn, and Al) in this core to be natural. Gradual increase in Cu, Zn, Mn, and Al concentration towards the surface along with lower organic carbon percentage therefore strongly suggested increase in marine inundation in recent years at this location.

Table 8 Range and average values of studied parameters within clay fraction of sediments

	Al (%)	Fe (%)	Mn (ppm)	Cu (ppm)	Zn (ppm)	Co (ppm)	Ni (ppm)	Pb (ppm)
Core S4								
Min	7.1	4.5	288	86.5	140	31	62	45
Max	12	12	857	164	239	91	119	95
Avg	9.3	6.9	576	124	176	48	104	74
Core S7								
Min	10.4	5.0	446	113	142	48	113	37
Max	12.3	6.7	1,556	154	233	75	164	178
Avg	10.4	5.9	920	135	178	59	138	97

Table 9 Correlation between metals in separated clay fraction

	Al	Fe	Mn	Cu	Zn	Co	Ni	Pb
Core S4								
Al	1.00							
Fe	*0.68*	1.00						
Mn	−0.42	−0.52	1.00					
Cu	*0.45*	0.24	−0.18	1.00				
Zn	*0.45*	0.33	−0.18	*0.61*	1.00			
Co	0.38	0.35	−0.03	*0.55*	0.39	1.00		
Ni	−0.16	0.28	0.03	−0.47	−0.25	−0.34	1.00	
Pb	0.05	0.18	0.17	0.04	0.20	−0.18	0.32	1.00
Core S7								
Al	1.00							
Fe	−0.07	1.00						
Mn	−0.51	−0.22	1.00					
Cu	−0.10	−0.21	−0.01	1.00				
Zn	−0.15	−0.19	−0.06	0.40	1.00			
Co	−0.52	−0.36	*0.61*	0.42	0.32	1.00		
Ni	−0.02	−0.28	0.20	0.33	0.05	0.43	1.00	
Pb	−0.07	−0.41	0.13	0.47	*0.65*	0.48	0.26	1.00

Marked correlations are significant at $p < 0.05$

While, presence of higher percentage of organic carbon, i.e., organic matter of terrestrial origin towards the bottom of core S9, seems to have diluted the metal concentration at greater depths. Organic matter of terrestrial origin must have been received during some flood event occurred in past probably as a result of heavy rainfall. Rainfall data of last hundred years was obtained from the Indian Meteorological Department, Pune. Rainfall data of three different stations of Thane district have indicated increase in rainfall approximately between years 1954 and 1961 (Fig. 8). Decreasing trend of Pb similar to that of organic carbon either suggested a common source or trapping

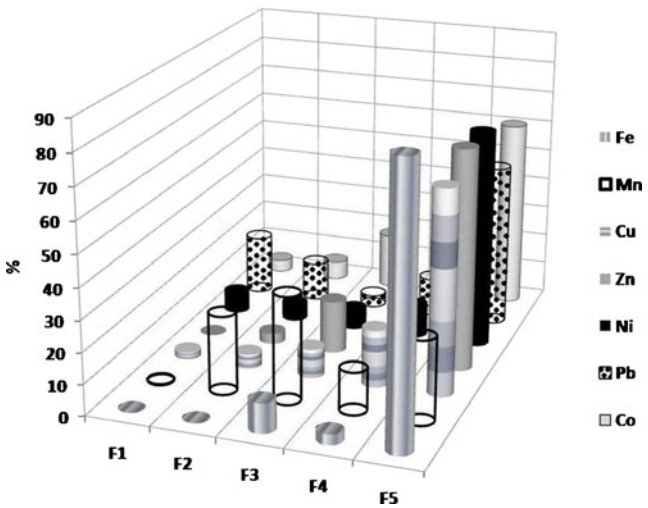

Fig. 9 Fractionation of metals in surface sediments of core S7

of Pb by organic matter or probably Pb have been introduced via organic materials (Du et al. 2008).

The higher concentration of Pb towards the bottom was probably a result of close association of Pb with humic (terrestrial) organic matter and sulfides (Rimmer 2004). Unlike core S9, cores S4 and S7 did not exhibit systematic variations, rather showed larger fluctuations in metal distribution with varying patterns from bottom to surface of the cores. Thus, indicating a whole range of processes and sources affecting their distribution pattern. While significant difference observed for almost all the metals between cores S4 and S7 was attributed to the difference in their physical environments.

The result of index of geoaccumulation (Tables 6 and 7) however indicated different levels of contamination for the studied metals in the sediments of Vaitarna estuary. All the studied metals seem to have been affected by anthropogenic activities in this estuary. Metals namely Pb, Co, followed by Cu showed the highest enrichment among the studied metals at the three locations. Among the three cores, core S7 indicated greater anthropogenic influence. The observed heavy metal contamination in sediments may therefore affect the water quality and bioaccumulation of metals in aquatic organisms, resulting in potential long-term implications on human health and ecosystem (Venkatramanan et al. 2012)

Bulk sediments represent metals which are associated with different sedimentary components. Clay-sized fraction of sediments represents last and stable weathering product or strong erosion of source rocks and mainly holds metals within lattice structure of alumino-silicate minerals. Thus represent metals which are least affected by anthropogenic processes unless they are associated with Fe-Mn oxyydroxides or organic matter which act as binding sites for metals or under excess metal availability for cation exhange. In the present study, Fe-Mn oxyydroxides and organic matter however showed no significant association with clay. Study of metals associated with clay fraction will therefore provide more detailed information on metals deposited within the estuary. Since cores S4 and S7 indicated influence of different sources and processes on metal distribution unlike in core S9, these two cores were studied for the clay chemistry to better understand processes controlling metal distributions.

Metals in clay fraction

When average concentrations of metals in clay fraction (Table 8) were compared with that in bulk sediments (Table 1), Zn and Pb were noted to be higher in clay fraction of both the cores while Cu and Ni were higher in clay fractions of cores S4 and S7, respectively. Fe, Mn, and Co concentration was

Table 10 Screening Quick Reference Table (SQUIRT) for metals in marine sediments (Buchman 1999)

Elements	Threshold effect level (TEL)	Effects range low (ERL)	Probable effects level (PEL)	Effects range median (ERM)	Apparent effects threshold (AET)
Fe	–	–	–	–	22 % (Neanthes)
Mn	–	–	–	–	260 (Neanthes)
Cu	18.7	34	108	270	390 (Microtox and Oyster Larvae)
Zn	124	150	271	410	410 (Infaunal community)
Co	–	–	–	–	10 (Neanthes)
Ni	15.9	20.9	42.8	51.6	110 (Echinoderm Larvae)
Pb	30.2	46.7	112	218	400 (Bivalve)

however higher in bulk sediments of both the cores as compared to the clay. Spatially, all the metals in clay fraction were higher in concentration in core collected towards the upper middle estuary (core S7) except for Fe. The higher concentration of Fe above 30 cm within core S4 (Fig. 4a), a peak value of Fe at 34 cm depth, and enrichment of Mn between 46 and 38 cm within core S7 (Fig. 6a) agreed with their similar increase within the bulk sediments and indicated diagenetic enrichment. Al concentration increased drastically above 30 and 18 cm depth of cores S4 and S7, respectively, where corresponding decrease within bulk sediment was noted. Metals, namely Cu, Zn, and Co in this fraction showed large increase in concentration above 22 cm depth of core S4 similar to that of Al. Correlation analysis had also shown strong positive association of these metals with Al (Table 9). Increase of metals above 22 cm depth in core S4 therefore suggested greater deposition of clay fraction bound metals in recent years. While in core S7, Zn, Co, Ni, and Pb showed a distinct peak at 30 cm depth. Mn also was noted to show slight enrichment at this depth. Sudden increase in metal concentration at greater depth strongly pointed towards their diagenetic enrichment. However, only Co showed strong positive correlation with Mn among these metals (Table 9). Cu, Zn, Ni, and Pb showed enrichment towards the surface of the core. While Zn and Pb showed strong positive association with each other, thus suggesting a common lithogenic source.

Together with anthropogenic additions such as domestic and agricultural wastes, sediments of Vaitarna estuary must be receiving abundant immature physically weathered materials (Jung et al. 2010) comprising of multitude of minerals such as altered pyroxene, amphiboles, and plagioclase feldspars containing a whole range of metals (Chang et al. 2007) as the source area consists largely deccan basalts. Clear identification of origin of metals whether natural or anthropogenic is of utmost importance. The observed variation in metal distribution between the bulk and separated clay sediment fraction in this study was therefore attributed to the complexity in the admixture of sediment particles and nonclastic chemical phases of the estuarine sediments (Padmalal and Seralathan 1995). According to Roussiez et al. (2006), all the trace metals may not be necessarily associated with the fine-grained alumino-silicates, but rather with the coarser silt fraction. This explains for the higher concentration of metals (Fe, Mn, and Co in both the cores and Ni in core S4) in bulk rather than clay fraction. Fe and Mn hydrous oxides and organic matter play important role in metal sorption onto the surfaces of clay minerals (Allen et al. 1990; Zhang et al. 2007; Sondi et al. 2008; Fernandes and Nayak 2009; Kumar and Edward 2009). The observed lower average concentrations of these metals within clay fraction was attributed to lower association of clay fraction with that of Fe-Mn oxyhydroxides as well as organic carbon.

Table 11 Sediment guidelines and terms used in SQUIRT

Sediment guidelines	
Threshold effect level (TEL)	Maximum concentration at which no toxic effects are observed
Effects range low (ERL)	10th percentile values in effects or toxicity may begin to be observed in sensitive species
Probable effects level (PEL)	Lower limit of concentrations at which toxic effects are observed
Effects range median (ERM)	50th percentile value in effects
Apparent effects threshold (AET)	Concentration above which adverse biological impacts are observed

Table 12 Metal concentration in bioavailable fraction per element

Elements	Metal concentration in bioavailable fraction (ppm)
Fe	8,114
Mn	670
Cu	59
Zn	24
Co	21
Ni	29
Pb	23

On the other hand, bulk sediments represent metals associated with crystal lattice structure of weathered minerals, as well as metals incorporated by surface sorption processes. This is further supported by good correlation observed between metals and relatively coarser size fractions in bulk sediments as well as results of speciation analysis (Fig. 9) carried out on surface sample of core S7 which was found to be most affected by anthropogenic activities in this estuary. The result of speciation analysis indicated all the studied metals except Mn to be mainly associated with residual fraction (Fig. 9), thus indicating lithogenic source as the main source of metals at this location. However, Mn and Co showed high bioavailability followed by risk of toxicity of Cu and Ni to sediment-dwelling organisms (Tables 10, 11, and 12). Fe concentration was much lower than AET, while Zn and Pb were noted to fall under TEL, thus were not harmful to the organisms. In the sediments of estuarine and near shore regions, iron oxide (hematite) occurs as a coating of 5–7 μm size around the coarser quartz and feldspar grains (Achyuthan et al. 2002). Such coatings must have facilitated the adsorption of metals onto the surfaces of relatively coarser sediments in the present study. In core S7, peak concentrations of trace metals at greater depth inferred diagenetic enrichment during the sediment deposition. The higher average concentration of Pb and Zn in clay fraction as compared to bulk sediments in both the cores was probably the result of their high retention capacity onto clay particles (Covelo et al. 2007; Vega et al. 2006). Smectite is the dominant clay mineral within the sediments of Vaitarna estuary. The study carried out by Ghayaza et al. (2011) has shown smectites to have a good capacity to retain Zn as well as Pb. Thus in the present study, Pb and Zn must have been competing successfully for the binding sites of finer particles as compared to the other metals leading to their observed enrichment within the clay fraction. Within Vaitarna estuary, the observed enriched concentrations of Pb and Zn therefore seem to be unaffected/least affected by anthropogenic activities as compared to other studied metals which have shown anthropogenic signatures.

Conclusions

Spatial and depth-wise variations in distribution of various parameters studied indicated variations in hydrodynamic energy conditions and depositional environments of Vaitarna estuary. Fe-Mn oxyhydroxide was the major sedimentary phase controlling the distribution of most of the metals in core collected towards the lower middle estuary as well as in core collected near the mouth. Greater deposition of clay fraction-bound metals in recent years was evident in core collected towards the mouth and must have been the result of increased marine inundation causing greater flocculation and deposition of metals and finer clay particles. Pb and Zn were found to be mainly associated with clay fraction and least affected by anthropogenic activities though higher in concentration. While most of the other metals showed greater enrichment in bulk sediments, indicating association with coarser particles and Fe-Mn oxyhydroxides, thus pointing towards their anthropogenic source in addition to that of lithogenic.

Acknowledgments One of the authors (Samida .P. Volvoikar) wish to thank the University Grants Commission for granting fellowship under the "Research Fellowships in Sciences for Meritorious Students" scheme. Our sincere thanks go to the India Meteorological Department for supplying the monsoon data.

References

Abrahim GMS, Parker RJ (2008) Assessment of heavy metal enrichment factors and the degree of contamination in marine sediments from Tamaki estuary, Auckland, New Zealand. Environ Monit Assess 136:227–238. doi:10.1007/s10661-007-9678-2

Achyuthan H, Richardmohan D, Srinivasalu S, Selvaraj K (2002) Trace metals concentrations in the sediment cores of estuary and tidal zones between Chennai and Pondicherry, along the east coast of India. Indian J Mar Sci 31(2):141–149

Allen JRL, Rae JE, Zanin PE (1990) Metal speciation (Cu, Zn, Pb) and organic matter in an oxic salt marsh, Severn estuary, Southwest Britain. Mar Pollut Bull 21(12):574–580

Aloupi M, Angelidis MO (2002) The significance of coarse sediments in metal pollution studies in the coastal zone. Water Air Soil Pollut 133:121–131

Álvarez-Iglesias P, Rubio B, Pérez-Arlucea M (2006) Reliability of subtidal sediments as "geochemical recorders" of pollution input: San Simón Bay (Ría de Vigo, NW Spain). Estuar Coast Shelf Sci 70:507–521

Attia OEA, Abu Khadra AM, Nawwar AH, Radwan GE (2012) Impacts of human activities on the sedimentological and geochemical characteristics of Mabahiss Bay, North Hurghada, Red Sea, Egypt. Arab J Geosci 5:481–499

Buchman MF (1999) NOAA screening quick reference tables. NOAA HAZMAT Report 99-1, (p 12). Seattle, WA, Coastal Protection and Restoration Division, National Oceanic and Atmospheric Administration

Caetano M, Prego R, Vale C, de Pablo H, Marmolejo-Rodríguez J (2009) Record of diagenesis of rare earth elements and other metals in a transitional sedimentary environment. Mar Chem 116:36–46

Chang M-L, Sun Y-C, Doong R-A, Wu S-C, Fu C-T (2007) Concentrations and correlations of trace metals in estuarine sediments—interpretation by multivariate statistical analysis and elemental normalization. J Env Eng Manage 17(2):143–150

Covelo EF, Vega FA, Andrade ML (2007) Simultaneous sorption and desorption of Cd, Cr, Cu, Ni, Pb, and Zn in acid soils I. Selectivity sequences. J Hazard Mater 147:852–861

Cundy AB, Croudace IW (1995) Sedimentary and geochemical variations in a saltmarsh/mudflat environment from the mesotidal Humble Estuary, southern England. Mar Chem 51:115–132

Dessai DVG, Nayak GN (2009) Distribution and speciation of selected metals in surface sediments, from the tropical Zuari estuary, central west coast of India. Environ Monit Assess 158:117–137

Dolch T, Hass HC (2008) Long-term changes of intertidal and subtidal sediment compositions in a tidal basin in the northern Wadden Sea (SE North Sea). Helgol Mar Res 62:3–11. doi:10.1007/s10152-007-0090-7

Du JZ, Mu HD, Song HQ, Yan SP, Gu YJ, Zhang J (2008) 100 years of sediment history of heavy metals in Daya Bay, China. Water Air Soil Pollut 190:343–351. doi:10.1007/s11270-007-9593-8

Fernandes L, Nayak GN (2009) Distribution of sediment parameters and depositional environment of mudflats of Mandovi estuary, Goa, India. J Coastal Res 25(2):273–284

Folk RL (1968) Petrology of Sedimentary rocks. Hemphills, Austin, p 177

Gaudette HE, Flight WR, Toner L, Folger DW (1974) An inexpensive titration method for the determination of organic carbon in recent sediments. J Sediment Petrol 44:249–253

Gazetteer of India, Maharashtra State Gazetteers, Thane District (Revised Edition) (1982) Bombay, Gazetteers Department, Government of Maharashtra

Ghayaza M, Le Forestier L, Muller F, Tournassat C, Beny J-M (2011) Pb(II) and Zn(II) adsorption onto Na- and Ca-montmorillonites in acetic acid/acetate medium: experimental approach and geochemical modeling. J Colloid Interface Sci. doi:10.1016/j.jcis.2011.05.028, 31p

Haris H, Aris AZ (2012) The geoaccumulation index and enrichment factor of mercury in mangrove sediment of Port Klang, Selangor, Malaysia. Arab J Geosci. doi:10.1007/s12517-012-0674-7

Huaiyang Z, Xiaotong P, Jianming P (2004) Geochemical characteristics and sources of some chemical components in sediments of Zhujiang (Pearl) river estuary. Chinese J Oceanol Limnol 22(1):34–43

Jonathan MP, Sarkar SK, Roy PD, Alam Md A, Chatterjee M, Bhattacharya BD, Bhattacharya A, Satpathy KK (2010) Acid leachable trace metals in sediment cores from Sunderban mangrove wetland, India: an approach towards regular monitoring. Ecotoxicology 19:405–418. doi:10.1007/s10646-009-0426-y

Jung H-S, Yun S-T, Choi B-Y, H-Mi K, Jung M, Kim S-O, K-Ho K (2010) Geochemical studies on the contamination and dispersion of trace metals in intertidal sediments around a military air weapons shooting range. J Soil Sediment 10:1142–1158. doi:10.1007/s11368-010-0248-9

Kljaković-Gašpić Z, Bogner D, Ujević I (2009) Trace metals (Cd, Pb, Cu, Zn and Ni) in sediment of the submarine pit Dragon ear (Soline Bay, Rogoznica, Croatia). Environ Geol 58:751–760. doi:10.1007/s00254-008-1549-9

Koretsky CM, Haveman M, Beuving L, Cuellar A, Shattuck T, Wagner M (2007) Spatial variation of redox and trace metal geochemistry in a minerotrophic fen. Biogeochemistry 86:33–62. doi:10.1007/s10533-077-9143-x

Koschinsky A (2001) Heavy metal distributions in Peru basin surface sediments in relation to historic, present and disturbed redox environments. Deep Sea Res Part II: Top Stud Oceanogr 48(17–18):3757–3777

Kumar SP, Edward JKP (2009) Assessment of metal concentration in the sediment cores of Manakudy estuary, south west coast of India. Indian J Mar Sci 38(2):235–248

Matini L, Moutou JM, Ongoka PR, Tathy JP (2011) Clay mineralogy and vertical distribution of lead, zinc and copper in a soil profile in the vicinity of an abandoned treatment plant. Res J Environ Earth Sci 3(2):114–123

Mukherjee D, Mukherjee A, Kumar B (2009) Chemical fractionation of metals in freshly deposited marine estuarine sediments of sundarban ecosystem, India. Environ Geol 58:1757–1767

Müller G (1969) Index of geoaccumulation in the sediments of the Rhine River. Geojournal 2:108–118

Nobi EP, Dilipan E, Thangaradjou T, Sivakumar K, Kannan L (2010) Geochemical and geo-statistical assessment of heavy metal concentration in the sediments of different coastal ecosystems of Andaman islands, India. Estuar Coast Shelf Sci 87:253–264

O'Reilly WSB, Bubb JM, Lester JN (1995) The significance of sediment metal concentrations in two eroding Essex salt marshes. Mar Pollut Bull 30(3):190–199

Ohmsen GS, Chenhall BE, Jones BG (1995) Trace metal distributions in two saltmarsh substrates, Illawarra region, New South Wales, Australia. Wetlands (Australia) 14:19–31

Padmalal D, Seralathan P (1995) Geochemistry of Fe and Mn in surficial sediments of a tropical river and estuary, India—a granulometric approach. Environ Geol 25:270–276

Pejrup M (1988) The triangular diagram for classification of estuarine sediments: a new approach. In: de Boer PL, Van Gelder A, Nios SD (Eds) Tide influenced sedimentary environments and facies. Reidel, Dordrecht, pp. 289-300

Rajkumar K, Ramanathan AL, Behera PN, Chidambaram S (2012) Preliminary studies on the characterization of clay minerals in the Sundarban mangrove core sediments, West Bengal, India. Arab J Geosci. doi:10.1007/s12517-012-0787-z

Rastogi BK, Mandal P, Kumar N (1997) Seismicity around Dhamni Dam, Maharashtra, India. Pure Appl Geophys 150:493–509

Rimmer SM (2004) Geochemical paleoredox indicators in Devonian-Mississippian black shales, Central Appalachian Basin, USA. Chem Geol 206:373–391

Roussiez V, Ludwig W, Monaco A, Probst J-L, Bouloubassi I, Buscail R, Saragoni G (2006) Sources and sinks of sediment-bound contaminants in the Gulf of Lions (NW Mediterranean Sea): a multi-tracer approach. Cont Shelf Res 26:1843–1857

Ruiz JM, Saiz-Salinas JI (2000) Extreme variation in the concentration of trace metals in sediments and bivalves from the Bilbao estuary (Spain) caused by the 1989–1990 drought. Mar Environ Res 49:307–317

Ruiz-Fernández AC, Hillaire-Marcel C, Páez-Osuna F, Ghaleb B, Caballero M (2007) ^{210}Pb chronology and trace metal geochemistry at Los Tuxtlas, Mexico, as evidenced by a sedimentary record from the Lago Verde Crater Lake. Quat Res 67:181–192

Ruiz-Fernández AC, Frignani M, Hillaire-Marcel C, Ghaleb B, Arvizu MD, Raygoza-Viera JR, Páez-Osuna F (2009) Trace metals (Cd, Cu, Hg and Pb) accumulation recorded in the intertidal mudflat sediments of three coastal lagoons in the Gulf of California, Mexico. Estuar Coast 32:551–564. doi:10.1007/s12237-009-9150-3

Sano T, Fujii T, Deshmukh SS, Fukuoka T, Aramaki S (2001) Differentiation processes of Deccan Trap basalts: contribution from geochemistry and experimental petrology. J Petrol 42(12):2175–2195

Sen G (2001) Generation of Deccan Trap magmas. P Indian AS-Earth 110(4):409–431

Shankar MNR, Mohan G (2006) Assessment of the groundwater potential and quality in Bhatsa and Kalu river basins of Thane district, western Deccan volcanic province of India. Environ Geol 49:990–998. doi:10.1007/s00254-005-0137-5

Shi Q, Leipe T, Rueckert P, Di Z, Harff J (2010) Geochemical sources, deposition and enrichment of heavy metals in short sediment cores from the Pearl River estuary, Southern China. J Mar Syst 82:S28–S42

Singh KT, Nayak GN (2009) Sedimentary and geochemical signatures of depositional environment of sediments in mudflats from a microtidal Kalinadi Estuary, Central West coast of India. J Coastal Res 25(3):641–650

Siraswar R, Nayak GN (2011) Mudflats in lower middle estuary as a favorable location for concentration of metals, west coast of India. Indian J Geo Mar Sci 40(3):372–385

Skowronek F, Sagemann J, Stenzel F, Schulz HD (1994) Evolution of heavy-metal profiles in river Weser estuary sediments, Germany. Environ Geol 24:223–232

Sondi I, Lojen S, Juračić M, Prohić E (2008) Mechanisms of land–sea interactions—the distribution of metals and sedimentary organic matter in sediments of a river-dominated Mediterranean karstic estuary. Estuar Coast Shelf Sci 80:12–20

Soto-Jiménez MF, Páez-Osuna F (2008) Diagenetic processes on metals in hypersaline mudflat sediments from a subtropical saltmarsh (SE

Gulf of California): postdepositional mobility and geochemical fractions. Appl Geochem 23:1202–1217

Spencer KL (2002) Spatial variability of metals in the inter-tidal sediments of the Medway Estuary, Kent, UK. Mar Pollut Bull 44: 933–944

StatSoft (1999) Statistica computer program, version 5.5. StatSoft, Tulsa, OK

Sullivan P, Taylor KG (2003) Sediment and pore water geochemistry in a metal contaminated estuary, Dulas Bay, Anglesey. Environ Geochem Health 25:115–122

Sundararajan M, Natesn U (2011) Environmental geochemistry of core sediments from Serthalaikkadu creek, East coast of India. Env Earth Sci 62:493–506

Swamy GN (1994) Training programme in Modeling and Monitoring of Coastal Marine Pollution (MAMCOMP), November 21–Dec 16, Lecture notes comp. by: Sinha P C. pp 591-593

Tessier A, Campbell PGC, Bisson M (1979) Sequential extraction procedure for the speciation of particulate trace metals. Anal Chem 51(7):844–851

Tribovillard N, Algeo T, Lyons T, Riboulleau A (2006) Trace metals as paleoredox and paleoproductivity proxies: an update. Chem Geol 232:12–32

Vega FA, Covelo EF, Andrade ML (2006) Competitive sorption and desorption of heavy metals in mine soils: influence of mine soil characteristics. J Colloid Interface Sci 298:582–592

Venkatramanan S, Ramkumar T, Anithamary I, Vasudevan S (2012) Heavy metal distribution in surface sediments of the Tirumalairajan River estuary and the surrounding coastal area, east coast of India. Arab J Geosci. doi:10.1007/s12517-012-0734-z

Venkatramanan S, Ramkumar T, Anithamary I (2013) Distribution of grain size, clay mineralogy and organic matter of surface sediments from Tirumalairajanar Estuary, Tamilnadu, east coast of India. Arab J Geosci 6:1371–1380

Wang G-P, Zhai Z-L (2008) Geochemical data as indicators of environmental change and human impact in sediments derived from downstream marshes of an ephemeral river, Northeast China. Environ Geol 53:1261–1270. doi:10.1007/s00254-007-0714-x

Wensink H (1973) Newer paleomagnetic results of the Deccan Traps, India. Tectonophysics 17:41–59

Williams TP, Bubb JM, Lester JN (1994) Metal accumulation within salt marsh environments: a review. Mar Pollut Bull 28(5):277–290

Zhang C, Wang L, Li G, Dong S, Yang J, Wang X (2002) Grain size effect on multi-element concentrations in sediments from the intertidal flats of Bohai Bay, China. Appl Geochem 17:59–68

Zhang W, Yu L, Lu M, Hutchinson SM, Feng H (2007) Magnetic approach to normalizing heavy metal concentrations for particle size effects in intertidal sediments in the Yangtze Estuary, China. Environ Pollut 147:238–244

Zwolsman JJG, Berger GW, van Eck GTM (1993) Sediment accumulation rates, historical input, postdepositional mobility and retention of major elements and trace metals in salt marsh sediments of the Scheldt estuary, SW Netherlands. Mar Chem 44:73–94

Zwolsman JJG, van Eck GTM, Burger G (1996) Spatial and temporal distribution of trace metals in sediments from the Scheldt estuary, south-west Netherlands. Estuar Coast Shelf Sci 43:55–79